Presented at "The 4th European Conference on Antennas and Propagation" (EuCAP 2010), Barcelona, Spain, 12-16 April 2010.

In-Flight Retrieval of Reflector Anomalies for the Planck Space Telescope

Frank Jensen*, Per Heighwood Nielsen*, Jan Tauber+, Arturo Martín-Polegre+

*TICRA
Laederstraede 34, 1201 Copenhagen, Denmark
fj@ticra.com, phn@ticra.com,

+ESTEC
Keplerlaan 1, 2200 AG Noordwijk, The Netherlands
Jan.Tauber@esa.int, Arturo.Martin.Polegre@esa.int

***Abstract*— It is important to know the antenna patterns for the Planck Space Telescope with high accuracy for detectors operating at frequencies from 30 to 857 GHz. This could not be achieved with sufficient accuracy on ground as the working temperature of the telescope is 40 K with the detectors cooled to 0.1 K. Accurate in-orbit measurements are thus requested.**

Simulations in which the reflector is displaced and the surface distorted with Zernike modes have been carried out for noise contaminated amplitude measurements of Jupiter by 5 and 10 different detectors. First, the main-beams of the antenna patterns are retrieved in a regular grid. Here the accuracy is limited by the noise level. Then, by a Physical Optics optimization the distortions of the telescope's reflector are determined so that the radiation patterns of the antenna are correlated to those measured. The patterns for the optimized, retrieved, reflector geometry are shown to be precise at levels far below the noise in the measurements.[1]

I. Introduction

The goal of the Planck Space Telescope is to observe the cosmic microwave background radiation with an unprecedented accuracy. It is therefore very important to know the patterns of the antenna with a correspondingly high accuracy. The Telescope is an aplanatic reflector system, Fig. 1, equipped with 47 microwave detectors in RF bands from 30 GHz to 857 GHz positioned over the curved focal 'plane' of the antenna, Fig. 2.

The antenna operates at very low temperatures: the reflectors, at 40 K, while the detectors operate at temperatures between 0.1K and 20K. On ground it has not been possible to test the antenna at temperatures lower than 40 K in the best case (i.e, for the smallest mirror), and these tests were surface and alignment tests, not RF tests. Some reflector deformations were identified, especially a hexagonal surface pattern caused by a print-through by the walls in the honeycomb core of the sandwich structure of the reflectors. At the even lower operating temperature, further reflector anomalies are foreseen and also the alignment of the parts of the system must be expected to be influenced.

The present paper describes the technique for in-flight testing of the antenna system. The Planck satellite is a spinning satellite, such that the antenna scans the full sky through six months. The beams of each detector then pass well-known celestial sources such as the planets Jupiter, Saturn, and Mars. These planets are mapped by all the Planck detectors when they are encountered during the course of regular observations. The maps obtained can be fitted to antenna models whereby reflector deformations and misalignments can be retrieved. Accurate beam patterns of each detector may subsequently be determined.

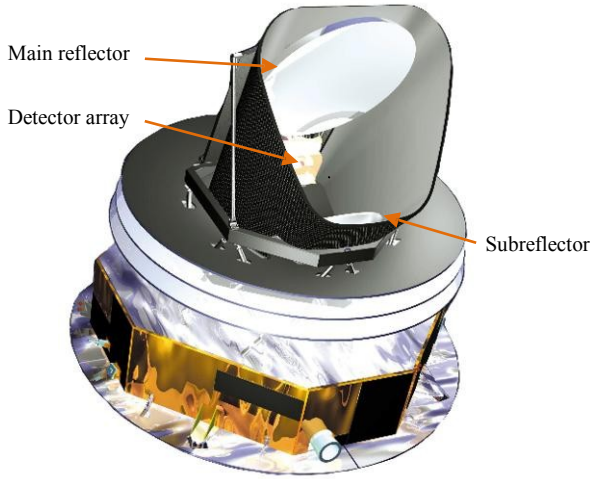

Fig. 1 The Planck satellite with the double reflector antenna surrounded by a baffle to protect against stray radiation. © ESA.

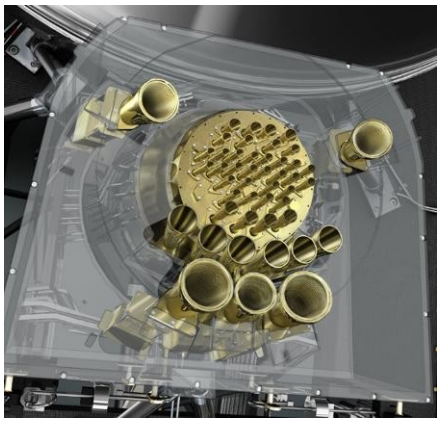

Fig. 2 The detectors of Planck in the focal region of the reflector system. © ESA.

[1] The work presented in the paper has been carried out under ESTEC Contract No. 18395/NL/NB

Because each detector probes a different frequency and a different location of the telescope's focal plane, each beam map contains redundant information related to the geometry of the system. The concept of the technique is to recover geometrical information from all detectors which is of higher quality than that recoverable from each detector by itself; and then to use this geometrical information to predict a beam pattern for each detector that is more precise than that recovered directly from the planet observations.

The high-precision antenna analyses are carried out by GRASP [1] and the pattern fitting is performed by Physical Optics applying a modified version of POS [2].

At the time of writing, in-flight measurements were not accessible and the technique is demonstrated on simulated measurements. The simulations are described in the following sections. First, in Section II, it is described how the scanning of a planet corresponds to a scanning of the antenna main beam and, in Section III, how a reliable beam pattern may be determined in a regular grid from the very irregularly distributed sampled points. The signals are contaminated by thermal noise. This is discussed in Section IV. In Section V simulations with deformed reflector surfaces are presented. Finally, the retrieval of the surface deformations of the reflectors is demonstrated in Section VI with the resulting accurate pattern determinations. The conclusions are drawn in Section VII.

II. Simulated Scan of Jupiter

The Planck satellite is positioned at Lagrange point L2 at which it may be kept stable with the shield at the 'bottom' towards the sun (cf. Fig. 1). The satellite spins by 1 rpm, and the spin axis is adjusted by 2 minutes of arc at each 2700 seconds (45 minutes) in order to keep the shield towards the sun but also to scan the full sky.

With Jupiter as example, the antenna beam will be scanned by the planet in cuts separated by 2 minutes of arc. In each scan, the beam will pass 45 times, and the signal from the planet will be sampled by the read-out frequency of the actual detector. The read-out frequencies range from 32.54 Hz for the 30 GHz LFI detectors – one of which will be considered in details in the following – to 200 Hz for the HFI detectors (100 – 857 GHz).

As an example, Fig. 3 shows the beam of the 30 GHz LFI-27 detector as a coloured contour plot. Overlaid are the positions of the sample points of a star sampled by the detector. Each sample point is presented by a red dot and the dots form vertical lines when these are swept 45 times until the spin axes is shifted 2 minutes of arc and a new line is sampled. With the given read-out frequency of the detector each vertical scan consists of 560 samples over the shown region.

The beam is given in uv-coordinates in the field-of-view coordinate system which is common for all detectors. The uv-coordinates are defined by

$$u = \sin(\theta)\cos(\varphi) \text{ and}$$
$$v = \sin(\theta)\sin(\varphi),$$

where θ and φ are usual spherical coordinates.

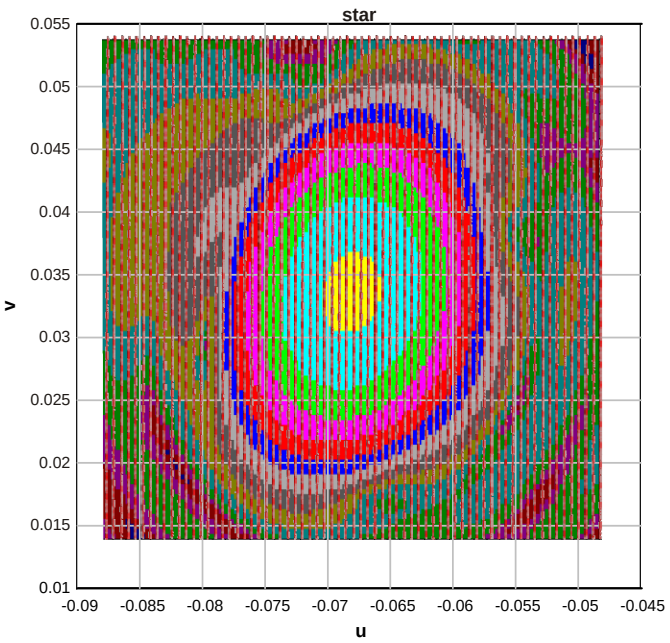

Fig. 3 Scan positions of a star (red dots forming vertical lines) over the main beam of the 30 GHz detector, LFI-27.

The complete scan of the beam shown consists of 69 vertical lines and will thus last about 52 hours. The movement of a planet during this time is not negligible. For Jupiter it is 11 minutes of arc, and must be taken into account. Further, the spin axis of Planck is nutating with a period of 6 minutes and a peak-to-peak amplitude in the range 0.4 to 2.8 minutes of arc. When these effects are included and Jupiter is drawn with its actual diameter the scans appear as shown in Fig. 4.

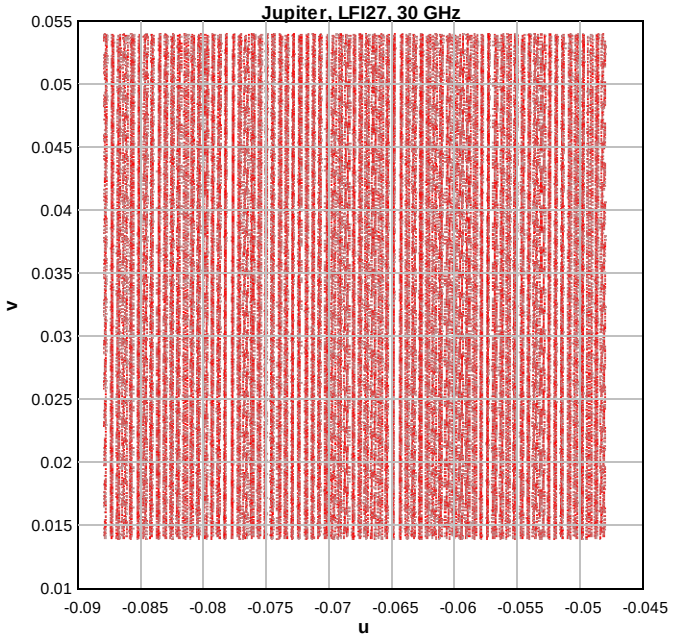

Fig. 4 In-flight measurements; scan directions with Jupiter as source for the 30 GHz detector, LFI-27.

III. First Determination of Detector Patterns

In order to plot and to further process the detector main beams from the observations of the planets, a special interpolation method has been developed. Hereby, the detector patterns are retrieved in a regular grid on the basis of which a standard interpolation for e.g. contour plots may be applied.

The observations, as those of Jupiter presented in the preceding section, are irregularly spaced with many observations in nearly the same directions and, further, with stochastic noise on the measured values. Therefore, an interpolation method passing through all observation points is not applicable.

Instead, a least square optimization is performed: The field values in the directions of a regular grid are the variable parameters with the measured signals in the measured directions as goals. The spacing in the regular grid shall be chosen according to the expected variations in the pattern. A reasonable choice spacing is thus 0.25 λ/D, where λ is the wavelength and D the diameter of the main reflector. The advantage of this method is that the influence of the stochastic noise is reduced and a smooth average pattern defined by fewer values is generated in the regular grid. This pattern may later be used for determination of the noise level in the measurements, cf. Section VI.

Neglecting noise, the pattern retrieved for the 30 GHz detector from observation of Jupiter in the directions of Fig. 4 is shown in Fig. 5. Compared to the correct pattern in Fig. 3, the deviations over the measured directions have an rms value of 0.4 dB only. The deviations are shown in Fig. 6. They have a maximum – 44 dB below main beam peak – in the side lobe region. In the main beam region the deviations are 70 dB below peak.

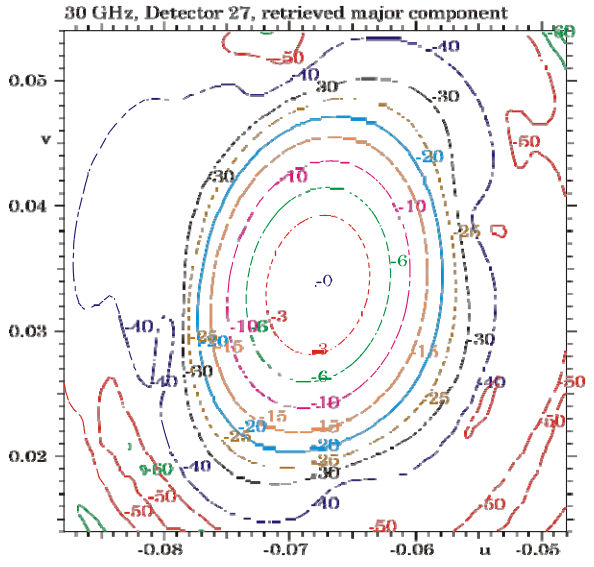

Fig. 5 Field pattern retrieved for the 30 GHz detector, LFI-27 under ideal circumstances (no noise, no reflector distortions). The peak maximum at 0 dB corresponds to 50.99 dBi.

As seen in the next section, these errors are insignificant compared to the noise in the measurements.

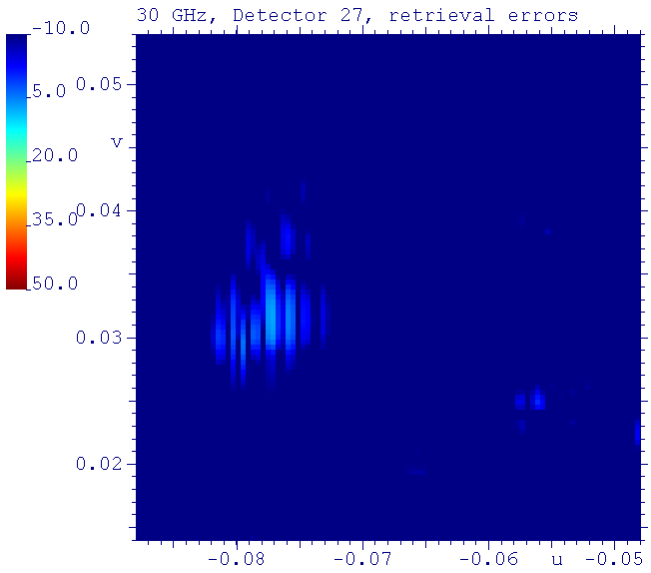

Fig. 6 Deviation of the retrieved field pattern from the correct pattern for the 30 GHz detector, LFI-27.

IV. Simulation of Noise

The noise in the measurements may be simulated for the various bands of the detectors according to the radiation characteristics of the sampled planet. For the 30 GHz detectors the level of the noise from Jupiter is determined to 33 dBi, 18 dB below peak.

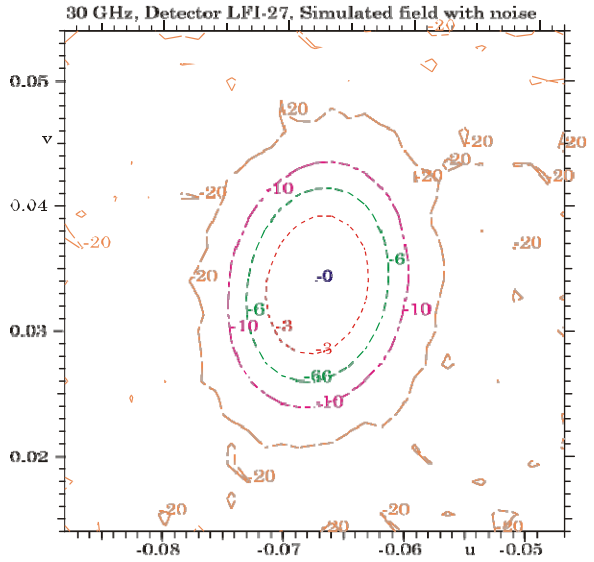

Fig. 7 Simulated field pattern with noise for 30 GHz detector, LFI-27. The peak maximum, 0 dB, is at 51.00 dBi.

The noise is introduced in the simulated data by adding a stochastic field amplitude, Gaussian distributed with the noise level being the 1σ level. The obtained retrieved pattern for the 30 GHz detector is shown as contour curves in Fig. 7 and in a 3D view in Fig. 8. Note that the actual error level is below 30 dBi due to the oversampling of the stochastic noise.

The patterns of Fig. 7 and Fig. 8 are used for determination of the level of the noise in the measurements. Hereby, meas-

urement values in which the noise is dominating may be discarded for the later processing.

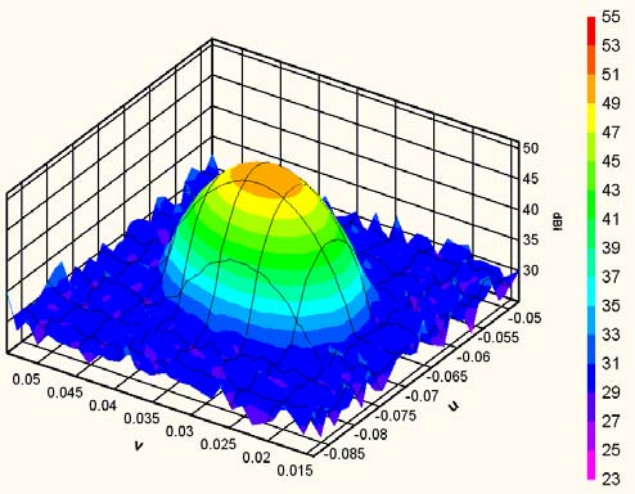

Fig. 8 Simulated field pattern with noise for 30 GHz detector, LFI-27. 3D view of the contour plot in Fig. 7.

V. Simulation of Reflector Distortions

In this section we will describe simulations of the influence of reflector distortions on the sampled signals. The distortions are expected to be small and will thus mainly affect the phase of the aperture field, not the amplitude. This means that it is difficult – and not important – to distinguish if the surface distortions belong to the sub- or the main reflector, and the simulations will be carried out for the latter.

The slowly varying distortions are simulated as a misalignment, consisting of a translation of the reflector to (x,y,z)=(1,1,1) mm, a rotation around the x-axis u_x=0.030º followed by a rotation around the y-axis u_y=0.057º. The y-axis is perpendicular to the plane of symmetry, cf. Fig. 1, and the x-axis is in this plane and perpendicular to the field-of-view direction. The fast varying distortions are simulated by two Zernike modes [3] with radial variation, (m,n) = (0,6) and (m,n) = (0,10), both with amplitude 0.01 mm at the edge of the reflector.

The main beams sampled without and with noise are shown in Fig. 9. Again, the noise level is at -18 dB, cf. Section IV. A comparison of the patterns without noise, Fig. 5 and Fig. 9(a), shows that the influence of the distortions is hard to see at levels above -30 dB, except for a general beam tilt appearing as a translation of the beam in the uv-plane. The level of the noise is at -18 dB which implies that the influence of the distortions is difficult to distinguish from the noise itself when the patterns with noise, Fig. 7 and Fig. 9(b), are compared.

VI. Retrieval of Reflector Distortions

In the retrieval of the reflector distortions it is advantageous to consider detectors farthest from the centre of the focal region as the patterns of these already possess a large inherent scan aberration which is perturbed by the distortions. Further, the retrieval is improved when beams measured at several frequencies are considered because the low frequencies reveal large as well as slowly varying surface deviations while the high frequencies correspondingly probe small and fast varying deviations.

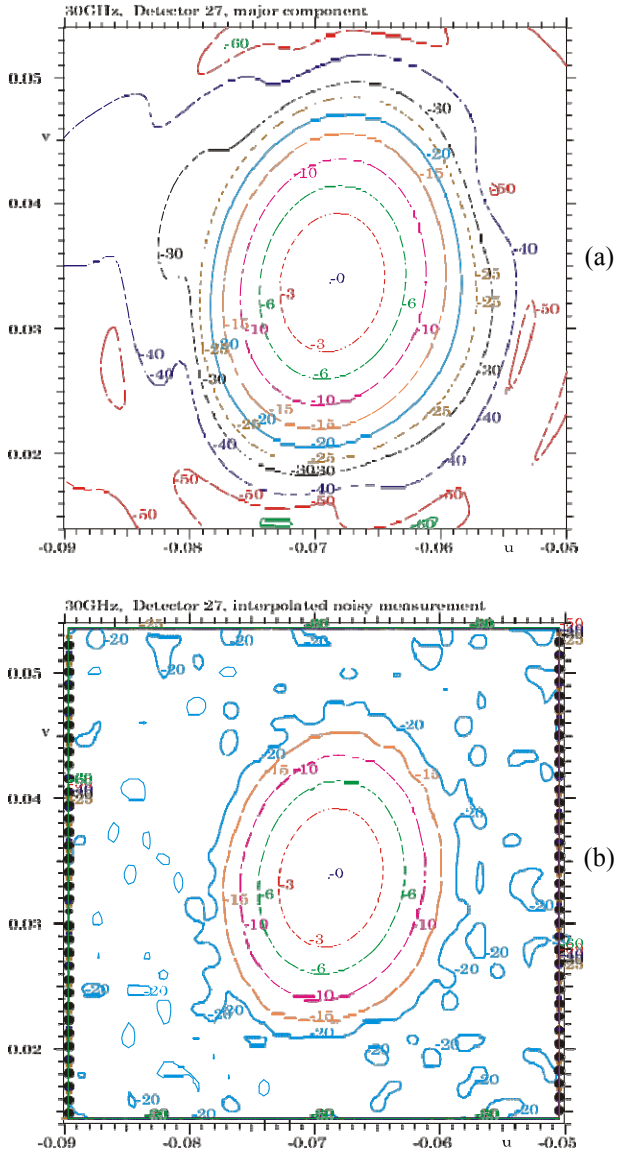

Fig. 9 Field pattern with simulated reflector distortions for the 30 GHz detector, LFI-27, without noise (a) and with noise (b).

The retrieval of the shape of the reflector surfaces is performed by an optimization in which surface perturbations described by Zernike modes are optimized in order to fit the given patterns. The field is determined by Physical Optics and the optimization is based on least squares deviation applying steepest descent for a fast optimization.

In the optimization the determined patterns are fitted to the measured patterns, but only within the regions in which the measured patterns are higher than a specified margin to the noise level found from the first, direct pattern determination, cf. Section III. Here, a margin of 6 dB is found appropriate.

The optimization is first carried out for 5 detectors marked as set 1 in Fig. 10, and next for 10 detectors by adding the detectors of set 2, Fig. 10.

The misalignments determined for these two cases are given in Table I together with the values of the introduced misalignments (in italics). When the retrieval is based on the 5 detectors of set 1, it is seen that the misalignment is reconstructed within 14% for translation of the reflector in the xy-plane, a movement which has only small influence on the antenna pattern and apparently the value of the translation is insignificant. In the case of the translation along z, the axis of the system is very accurately predicted because an axial defocusing changes the width of the beam. The rotation of the reflector is predicted within 10%. When detector set 2 is included in the retrieval, the predictions are improved to 12% and 7%, respectively.

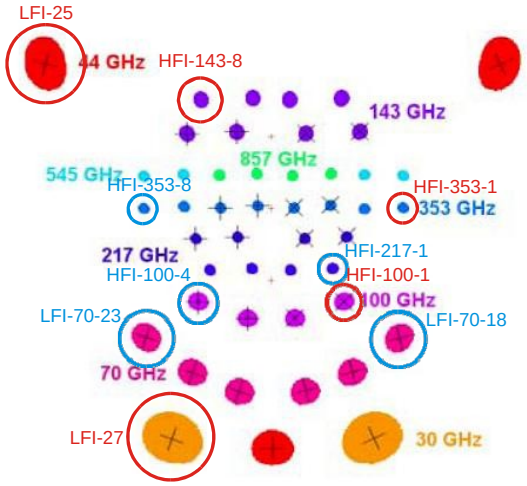

Fig. 10 The footprints of the detectors of set 1 are circled in red, and those of set 2 are circled in blue, cf. Fig. 2 for the layout of the detectors.

TABLE I
INTRODUCED AND DETERMINED ALIGNMENT ERRORS

Misalignment	**(x,y,z) [mm]**	**u_x**	**u_y**
Introduced	*(1.,1.,1.)*	*0.03000º*	*0.05700º*
Found, set 1	(0.860,1.107,0.993)	0.03317º	0.05483º
Found set 1+2	(0.881,1,076,0.991)	0.03220º	0.05506º

The determined surface distortions are presented in Table II. The Zernike modes (0,6) and (0,10) are 0.004 mm and 0.002 mm from the correct value, respectively, when the retrieval is based on the detectors of set 1. Unfortunately, the low order generated modes are of the same size and adding the detectors of set 2 does not improve the determined values.

TABLE III
INTRODUCED AND DETERMINED REFLECTOR DISTORTIONS

Zernike mode (m,n)	**(0,2)**	**(0,4)**	**(0,6)**	**(0,8)**	**(0,10)**
	Amplitudes at edge [mm]				
Introduced	*0.*	*0.*	*0.010*	*0.*	*0.010*
Set 1	0.014	0.010	0.014	-0.001	0.008
Set 1+2	0.012	0.010	0.019	0.006	0.012

Nevertheless, the patterns predicted on basis of the retrieved surfaces are very good as seen in Fig. 11 which shows the pattern of the antenna with the retrieved antenna distortions (based on the results applying 10 detectors) together with the pattern of the measured, distorted antenna. The deviation between the two patterns is more than 58 dB below peak, 40 dB lower than the noise level at 18 dB below peak. This considerable improvement is due to the measurements up to 353 GHz for which the simulated distortions are slowly varying and influencing the main beam at levels above the noise.

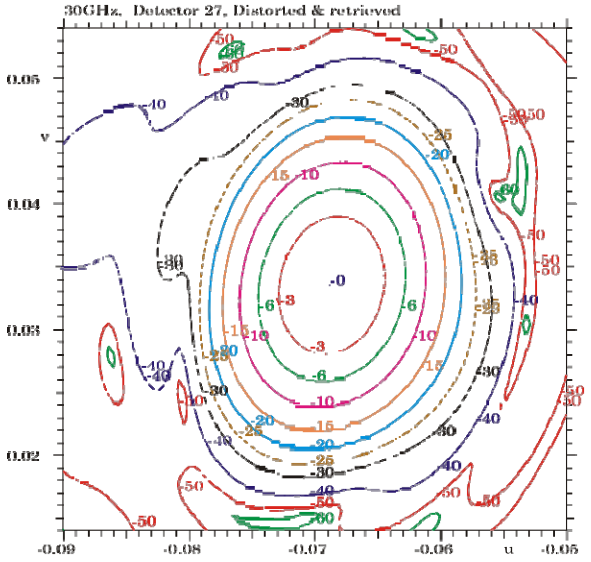

Fig. 11 Field pattern for the 30 GHz detector, LFI-27 determined from the retrieved reflector distortions. Overlaid is the correct pattern of the distorted antenna, cf. Fig. 9(a).

VII. CONCLUSION

By Simulations it has been demonstrated that the patterns of the antenna on the Planck satellite may be retrieved with high accuracy after the satellite is placed in orbit.

As the satellite is scanning the sky, the antenna will also scan the planets and as a first step it has been demonstrated how the antenna pattern may be determined by a least squares fitting to the measured data points. With Jupiter as example it is shown that this pattern can be determined a few dB below the noise level due to the considerable oversampling.

However, much better results are obtained when measurements from several of the detectors are applied to retrieve the surface distortions of the common reflectors. On the basis of these predicted surface distortions it is found possible to determine the field accurately down to about 40 dB below the noise level.

In order to further improve the accuracy of the retrieval it is planned to represent the surface distortions by spline functions instead of by Zernike polynomials which inconveniently have their maximum along the rim of the reflector.

REFERENCES

[1] K. Pontoppidan, *GRASP9 Technical Description*, Copenhagen, Denmark: TICRA, 2005. May be downloaded from the TICRA website [Online]. Available: www.ticra.com > FreeDownloads > GRASP-SE

[2] The TICRA website. [Online]. Available: www.ticra.com > What We Do > Software Descriptions > POS

[3] M. Born and E. Wolf, *Principles of Optics*, 6th (corrected) ed., Oxford, UK: Pergamon Press, 1983.c